*Present address: Basler and Hofmann, 8008 Zürich, Forchstrasse 395, Switzerland.

[1]F. Steinrisser and E. N. Sickafus, Phys. Rev. Letters 27, 992 (1971).

[2]The expressions $N(E)$, $N(E,E_p)$, and $N(E_p-E_L,E_p)$ are equivalent, as is $N(E_L, E_p)$ following a transformation of coordinates given by $E=E_p-E_L$. When an emphasis on parametric features is desired either $N(E_L)\mid_{E_P}$ or $N(E_p)\mid_{E_L}$ is used.

[3]E. Sickafus, Rev. Sci. Instr. 42, 933 (1971).

[4]C. Davisson and L. H. Germer, Phys. Rev. 30, 705 (1927).

[5]J. C. Turnbull and H. E. Farnsworth, Phys. Rev. 54, 509 (1938). $N(E_L)\mid_{E_P}$ and $N(E_p)\mid_{E_L}$ curves apparently were first published by these authors. They examined only narrow-apertured spectra centered on the specular beam which, consequently, did not permit simultaneous examination of all active elastic channels.

[6]C. B. Duke, A. J. Howsmon, and G. F. Laramore, J. Vacuum Sci. Tech. 8, 10 (1971).

[7]J. O. Porteus, *Structure and Chemistry of Solid Surfaces*, edited by G. A. Somorjai (Wiley, New York, 1969), pp. 12-1.

[8]A dynamical theory of diffraction has been applied on DL, LD, and DLD processes by Duke and Landman [Phys. Rev. B (to be published)] for the case of energy loss due to excitation of bulk plasmons and surface plasmons.

[9]E. N. Sickafus and H. P. Bonzel, Progr. Surface Membrane Sci. 4, 181 (1970).

[10]J. C. Gregory, Bull. Am. Phys. Soc. 15, 1326 (1970); J. C. Gregory and D. O. Hayward, *Structure and Chemistry of Solid Surfaces*, edited by G. A. Somorjai (Wiley, New York, 1969), pp. 56-1.

[11]E. N. Sickafus, Surface Sci. 19, 181 (1970).

[12]R. V. Stuart and G. K. Wehner, J. Appl. Phys. 33, 2345 (1962).

[13]B. Heimann and J. Hölzl, Phys. Rev. Letters 26, 1573 (1971).

[14]H. Raether, *Springer Tracts in Modern Physics*, edited by G. Höhler (Springer-Verlag, Berlin, 1965), Vol. 38, pp. 84–157.

[15]J. G. Hanus, MIT Solid State and Molecular Theory Group Quarterly Report, No. 44, 1962 (unpublished).

[16]C. J. Powell, J. Opt. Soc. Am. 59, 738 (1969).

PHYSICAL REVIEW B VOLUME 6, NUMBER 10 15 NOVEMBER 1972

Anomalous Electrical Resistivity in Titanium-Molybdenum Alloys*

J. C. Ho† and E. W. Collings
Columbus Laboratories, Battelle, Columbus, Ohio 43201
(Received 11 May 1972)

The results of resistivity measurements on Ti-Mo alloys of concentrations 5–20 at.% Mo are discussed. The experimentally determined *resistivity concentration dependence*, which exhibits a pronounced local maximum near 8 at.% Mo, is compared with some calculated curves, derived with the aid of previously determined Fermi-density-of-states $[n(E_F)]$ and Debye-temperature (Θ_D) data. On the assumption that the total resistivity is the sum of contributions due to thermal scattering (the ideal resistivity ρ_i) and solute scattering (ρ_s), the measured resistivity in the concentration range 5–15 at.% Mo is shown to be anomalously high. For a quenched alloy of composition near the middle of the above range, viz., Ti-Mo (10 at.%), the *temperature dependence* of resistivity ($d\rho/dT$) is negative between 4 and 480 K. But at higher temperatures $d\rho/dT$ is positive, and after being aged at 620 K the alloy assumes a normal positive $d\rho/dT$ over the full temperature range of 4–620 K. As a result of this investigation it is deduced that the anomalous magnitude, composition dependence, and temperature dependence are all associated in one way or another with an ω-phase precipitate (a small fraction of which is reversible or "athermal") occurring in the brine-quenched alloys within the composition range 5–15 at.% Mo. It is concluded, however, that the observed resistivity effects do not derive from intrinsic physical properties of the ω phase itself, but are due instead to electronic scattering from the interfaces between the precipitate particles and the matrix. Interfacial scattering associated with the irreversible (isothermal) ω phase is responsible for the anomalous isothermal resistivity, while the relatively small athermal ω-phase component gives rise to the negative $d\rho/dT$ exhibited by Ti-Mo (10 at.%).

I. INTRODUCTION

In a comprehensive study of the physics of the Ti-Mo system, as a representative of Ti-base transition-metal binary (Ti-T_2) alloys in general, we have investigated the manner in which electronic properties are influenced by metallurgical microstructure and microstructural change. As a guide to the discussion which follows, a pair of phase diagrams for Ti-Mo is presented [Figs. 1(a) and 1(b)] together with a diagram [Fig. 1(c)] indicating the structures found and estimated to be present in 30-g alloy ingots which had been quenched from elevated temperatures into iced brine. Figure 1(c) makes reference to an ω phase. This is a microscopic or submicroscopic precipi-

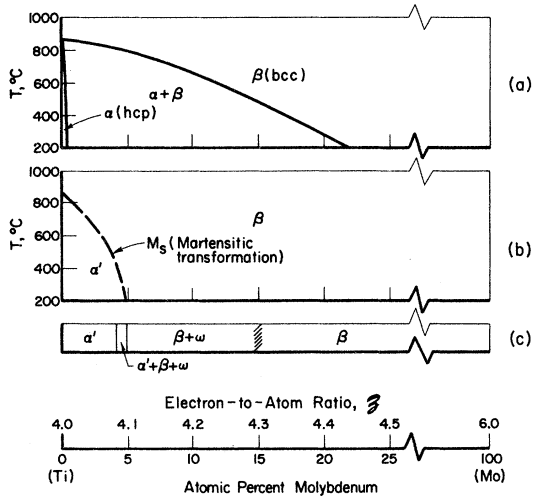

FIG. 1. (a) Part of the equilibrium phase diagram for Ti-Mo. (b) Structures assumed by Ti-Mo alloys upon being quenched from elevated temperatures (say > 900 °C) to temperatures indicated on the scale. Because its occurrence depends on the quench rate and/or subsequent moderate-temperature (~ 350 °C) annealing, ω phase is not indicated in this diagram. (c) Structures observed, or deduced, to be present in 30-g ingots quenched into iced brine. ω-phase precipitation "fades out" in the composition range 10–15 at.% Mo. The quenched structures in Ti (transition-metal) alloys are generally a function of the average valence ($s+d$) electron-to-atom ratio z, indicated in the scale at the foot of the figure.

tate, hexagonal in crystal symmetry, which can be expected to be present in as-quenched Ti-T_2 alloys in the appropriate concentration range, as discussed in the caption to Fig. 1.

As part of the physical-property investigations, we measured the concentration dependence of electrical resistivity in a limited series of Ti-Mo alloys, finding a pronounced local maximum near 8 at.% Mo. The temperature dependences of resistivity ($d\rho/dT$) were also measured. Of particular interest here was the observation of a negative $d\rho/dT$ in Ti-Mo (10 at.%). Such behavior, which several workers[1,2] had already reported seeing in Ti-Mo, is undoubtedly related to those noted in other Ti-T_2 alloys (where T_2 = V,[3] Cr,[4] Nb[5]) and in Zr-Nb.[6] These negative $d\rho/dT$'s all occurred within concentration ranges which we now know to favor the precipitation of the ω phase.[7–10] For this reason we selected for the resistivity study alloys of compositions 5–20 at.% Mo, thus spanning the region of ω-phase precipitation in the Ti-Mo system. Particular attention was given to Ti-Mo (10 at.%), the central member of the series, which yielded copious amounts of ω phase during ice-brine quenching and in which the subsequent development of the precipitate could be conveniently controlled by heat treatment.[10]

II. EXPERIMENTAL DETAILS

A. Specimen Materials

Six Ti-Mo (5–20-at.%) specimens, herein designated TM-5, -7, -10, -15, -16, and -20, were cut from well-homogenized (multiply melted) arc-melted ingots prepared from high-purity Ti and Mo. The principal impurities in the starting materials are listed below,[11] and the chemically analyzed compositions of the ingots are given in Table I.

B. Experimental Techniques

Resistivity measurements were carried out, using the four-probe dc method, on specimens about 1 in. in length, which had been ground to rectangular cross sections of about 0.1×0.1 in.[2] Current was supplied by a 12-V accumulator and regulated by a Tinsley current regulator (type

TABLE I. Results of present measurements of electrical resistivity and resistivity temperature dependence (4–300 K) in some Ti-Mo alloys (0–20 at.% Mo).

Alloy	Analyzed composition[a] (at. %Mo)	Heat treatment	Electrical resistivity ρ ($\mu\Omega$ cm) 300 K	78 K	4.2 K	Resistivity temperature dependence $\rho_{300\,K} - \rho_{4K}$
hcp Ti	...	as-cast	47.8	5.2_2	1.6_8	+46
TM-5	5.09	1000 °C, 8 h, IBQ[b]	137	112	107	+30
TM-7	6.86	1000 °C, 8 h, IBQ	149	149	149	0
TM-10	10.30	1200 °C, 2 h, IBQ	138	146	148	−10
TM-15	14.92	1200 °C, 2 h, IBQ	120	120	120	0
TM-16	16.59	1200 °C, 2 h, IBQ	117	115	112	+5
TM-20[c]	19.38	1200 °C, 2 h, IBQ	118	111	110	+8

[a]"Wet" chemical analysis. These specimens of TM-5, -7, and -16 were prepared especially for the resistivity work, hence the compositions of these TM-5 and -7 alloys differ slightly from those listed in Table III.

[b]Anneal abruptly terminated by quenching of the specimens into iced brine (IBQ).

[c]Assuming $\rho_{4K} = \rho_{0K}$, then $\rho_{i,\,300\,K} = 8\ \mu\Omega$ cm. With the same assumption, $\rho_s = \rho_{4K} = 110\ \mu\Omega$ cm.

5390) capable of delivering a constant 0.1, 0.5, 1.0, or 2.0 A into any low-resistance load. The potential readings were taken with either a Kiethley model No. 147 nanovoltmeter, or a Leeds and Northrup K3 potentiometer, to a precision (during a temperature-dependence measurement) of about ±1%. The accuracy of resistivity measurements is estimated to be about ±4%, the principal limitations being the usual uncertainties inherent in determining the dimensions of the specimens, and the separations of the potential probes.

Prior to commencing the resistivity study, the specimens were annealed for 8 h at 1000 °C (TM-5 and -7), or for 2 h at 1200 °C (TM-10, -16, and -20), and quenched into iced brine. The forms and compositional ranges of the resulting microstructures [Fig. 1(c)] were assumed to correspond to those of the previously quenched parent (30-g) ingots, whose structural and physical properties had already been studied in some detail[12–17] and which had been subjected to heat treatments equivalent to those administered here. The resistivity program was carried out in three stages:

(i) Measurements were made on each of the six alloys from room temperature (nominally 300 K) to 4.2 K, and, in a search for possible hysteresis of the resistivity temperature dependence, the temperature was cycled five times within this range.

(ii) In a second phase of the work TM-10, -15, -16, and -20 were sealed under argon in a leak-tight Vycor tube, and resistivity measurements were taken as the vessel and contents were heated to 620 K during a period of about 30 min.

(iii) Finally, these four specimens were held at 620 K for about 160 h before being cooled to 4.2 K. Resistivity measurements were made at suitable intervals throughout the heat treatment and subsequent cooling.

III. RESULTS AND DISCUSSION

A. Isothermal Composition Dependence of the Resistivity—Comparison with Earlier Investigations

Although we were interested primarily in the resistivity temperature dependences of the alloys, so that precision was more important than accuracy, it is reassuring to find that our value for pure hcp Ti (47.8 $\mu\Omega$ cm at 300 K) was in satisfactory agreement with those reported by Ames and McQuillan[5] (45 $\mu\Omega$ cm[18]), Wasilewski[19] (47.8 $\mu\Omega$ cm at 300 K), and Hake *et al.*[2] (47 $\mu\Omega$ cm at 300 K[20]). The resistivity composition dependences at temperatures 4.2, 78, and 300 K for TM(5–20) are listed in Table I and displayed in Fig. 2. In spite of a systematic difference of less than 10%, which might be partly attributable to differing heat treatments,[21] our results are in reasonable agreement with those of Hake *et al.*,[2] in that both sets of curves show pronounced negative composition dependences ($d\rho/dc$) in the range of about 8–18 at.% Mo. By extending the composition range of the measurements to include TM-5 we were able to demonstrate that the negative $d\rho/dc$ did not persist below about 8 at.% Mo, but that it seemed to represent the high-concentration part of an excess-resistivity anomaly centered on Ti-Mo (8 at.%). Noting the manner in which the isotherms intersect in Fig. 2 we see that the resistivity maxima occur within a region (7–15 at.%) of negative-resistivity temperature dependence.

Figure 3 is included as a representative of the earliest resistivity experiments[5] on Ti-T_2 alloys. As in Fig. 2, a scale of average electron-to-atom ratio $\mathfrak{z}$ is included, since that quantity is a reasonably good describer of the kinds of microstructure to be expected in quenched Ti-T_2 alloys [cf. Fig. 1(d)]. The results shown in Fig. 3 are in good accord with those of the Ti-Mo experiments, in the sense that for $\mathfrak{z} \lesssim 4.3$ the resistivity isotherms cross and enter a region of negative $d\rho/dT$ as ρ begins to increase rapidly with decreasing solute concentration. It would be instructive to extend the data of Fig. 3 at least down to Ti-Nb (~15 at.%), where we would expect $d\rho/dT$ to vanish once more.

Comparing Fig. 2 with Fig. 1(c) we see that the resistivity maximum near $\mathfrak{z} = 4.1_6$ occurs within the $\beta+\omega$ regime. Furthermore, the rather abrupt drop in resistivity on the low-concentration side might very well be the result of partial martensitic transformation (to "α'"). Such a hexagonal-based structure with its relatively low Fermi density of states $n(E_F)$ (e.g., Refs. 12, 14, and 22) would be expected to have a lower ideal resistivity than the cubic.

Evidence in support of an apparent negative $d\rho/dc$ in β-Ti-T_2 alloys has been presented by previous workers (e.g., Refs. 2 and 5) in at least two different ways:

Model (*a*). Following Ames and McQuillan[5] the ρ-c curves for concentrated Ti-V and Ti-Nb alloys can be extrapolated back so as to intersect the ρ axis at resistivities near 140 $\mu\Omega$ cm [in good accord with those values (viz., 132[5] and 134.7 $\mu\Omega$ cm[19]) obtained by extrapolating ρ-T for elevated-temperature pure β-Ti ($T > 885$ K) back to 300 K]. The resulting practically straight lines, assumed to be appropriate to β-Ti-T_2, possess negative slopes.

Model (*b*). On the other hand, Hake *et al.*[2] in a later investigation focused attention on those few alloys whose resistivities fall on what we now recognize as the high-concentration side of an excess-resistivity maximum.

These two representations of negative $d\rho/dc$ are illustrated, with respect to Ti-Mo, in Fig. 4 [curves (a) and (b), respectively]. In model (a) the negative slope of the dashed line might be regarded as being consistent with a high value for $\rho(\beta\text{-Ti})$, were it stable at 300 K, followed by monotonically decreasing ideal resistivities for β-Ti-Mo alloys, were they also stable at 300 K. But this may not be a valid representative since great caution must be exercised in interpreting results obtained by extrapolation into a regime of structural instability. In Ti-Mo we contend that such extrapolations of physical properties appropriate to β-phase alloys are meaningful down to $\mathfrak{z} \cong 4.1$, but not necessarily so below that value. Turning now to model (b), it is significant that the compositional range containing the resistivity maximum coincides with that which encourages ω-phase precipitation in the quenched alloys, suggesting that the observed negative $d\rho/dc$ is, in fact, a result of the presence of ω phase rather than some property of single-phase β-Ti-Mo.

It is, therefore, important, in this context, to inquire whether the anomalously high resistivity is associated with the particular electronic and lattice-vibrational properties of the ω phase itself.

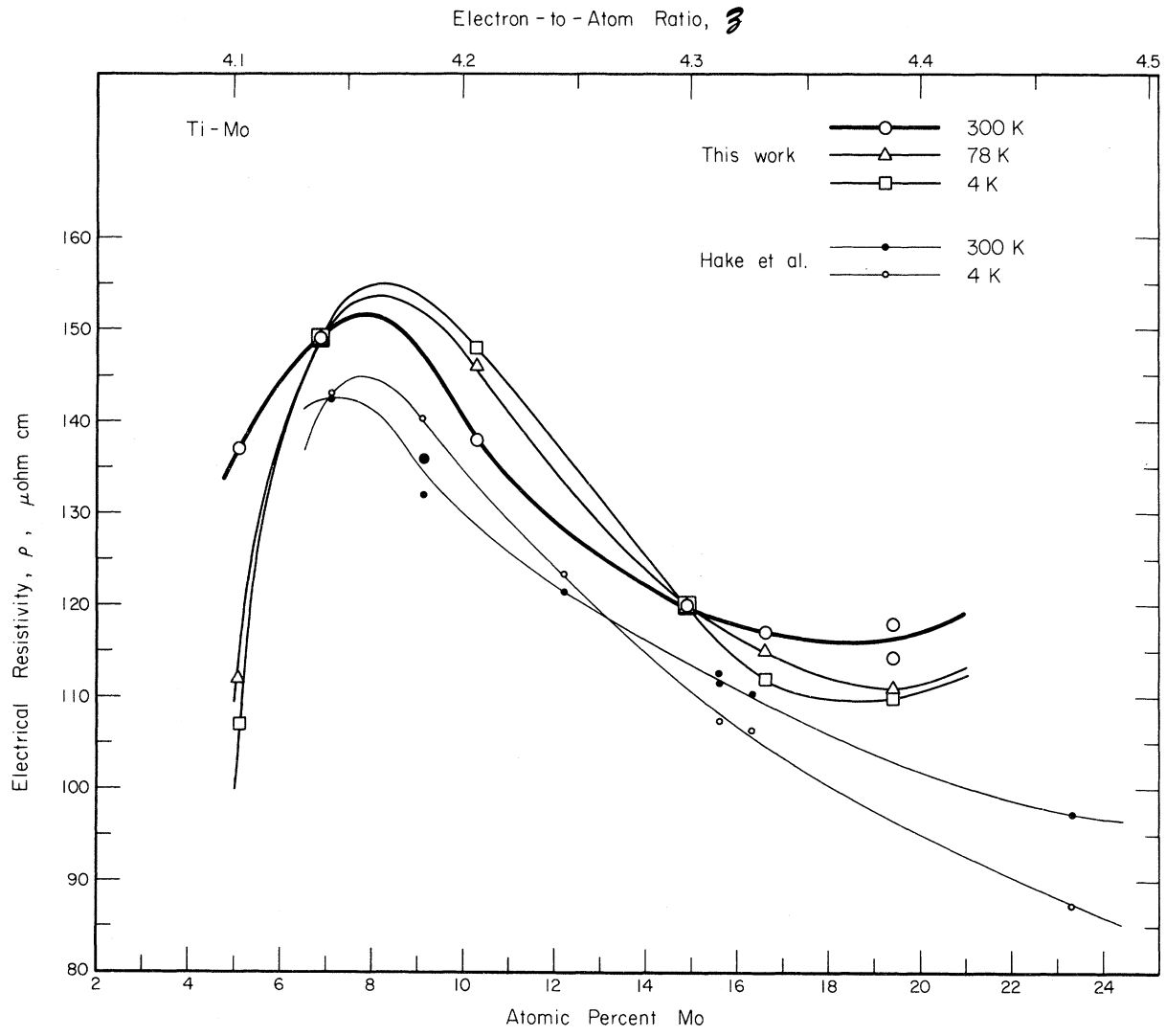

FIG. 2. Composition dependence of resistivity (ρ-c) of quenched Ti-Mo, measured at temperatures nominally 4, 78, and 300 K (i.e., room temperature). TM-20 was first measured as $117._6 \mu\Omega$ cm and subsequently (15 months later) as $114._4 \mu\Omega$ cm; we therefore feel that the local minimum occurring between 16 and 20 at.% Mo is real. It is certainly consistent with the behavior of the calculated resistivity at higher Mo concentrations (Fig. 6). Shown for comparison are the results of measurements by Hake *et al.* (Ref. 2) on some as-cast Ti-Mo alloys. The two sets of data share the following important characteristic: a region of negative $d\rho/dT$ on the high-concentration side of a local ρ-c maximum.

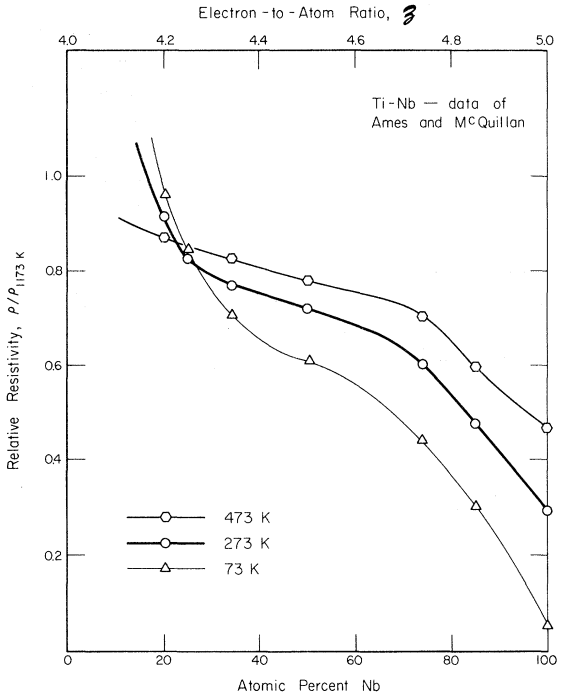

FIG. 3. Resistivity-composition curves for Ti-Nb alloys from the early work of Ames and McQuillan (Ref. 5). As in the previous figure the resistivity isothermals cross over into a region of negative $d\rho/dT$ as the solute concentration decreases. Magnetic susceptibility studies of both as-cast and quenched Ti-Nb recently carried out in this laboratory indicate that the physical properties are strongly influenced by the presence of ω phase, particularly within the composition range 15–25 at.% Nb. We suggest that both the anomalous $d\rho/dc$ and the anomalous $d\rho/dT$ could be traced to influences of "isothermal" and "athermal" ω phase (Ref. 31), respectively.

Accordingly, we proceed to calculate the resistivities of the β-phase and $(\beta+\omega)$-Ti-Mo alloys with the aid of some experimental data determined from a series of low-temperature specific-heat and magnetic susceptibility measurements.[14,22]

B. Isothermal Composition Dependence of the Resistivity—Comparison with Calculated Resistivities

1. Theoretical Model for Total Resistivity

The total resistivity is expressible as the sum of contributions due to scattering by lattice thermal vibrations (the "ideal resistivity" ρ_i), by solute atoms (ρ_s), and by static lattice defects (ρ_{def}). Mott and Jones[23] in discussing the resistivities of alloys containing transition elements have pointed out that s-d scattering, assumed to be proportional to the Fermi density of d states $[n_d(E_F)]$, could make a significant contribution to the resistivity. In accordance with this Chandrasekhar and Hulm[24] have suggested that ρ_s, for an alloy in which electron scattering into d states is the dominant mechanism, should be expressible as

$$\rho_s \propto n_d(E_F)c(100-c), \tag{1}$$

where c is the solute concentration in at.%. For most Ti-T_2 alloys $n_d(E_F)\cong n(E_F)$, the total $(s+d)$ Fermi density of states.

Hake *et al.*[2] pointed out that Eq. (1) could not explain the observed negative $d\rho/dc$ since (then) contemporary calorimetric evidence[25] had indicated that $n(E_F)$ *increased* with increasing c in the region of interest, viz., $4.1 < z < 4.3$. We have confirmed this property of quenched Ti-Mo alloys, but have also shown[14] that, were it not for the presence of ω phase, $n(E_F)$ for β-Ti-Mo would otherwise *decrease* monotonically as z increased from 4.1 to 6.0 (pure Mo). This property of $n(E_F)$ will be referred to later in connection with the ρ_i component of alloy resistivity. But, of course, Eq. (1) is still incapable of yielding a negative $d\rho/dc$ in the Ti-rich region since the concentration dependence of ρ_s is controlled by the factors $c(100-c)$.

On the other hand, ρ_i, which remains finite throughout, could conceivably yield the required excess resistivity. The ideal resistivity is most simply expressed as

$$\rho_i = mv_F/ne^2\Lambda_i,$$

where m and e are the mass and charge, respectively, of the conduction electrons of density n per unit volume, v_F is the Fermi velocity, and Λ_i is the mean free path controlled by thermal scattering processes. Rewriting in terms of the Fermi density of states, we have

$$\rho_i \propto n(E_F)/n\Lambda_i\ . \tag{2}$$

It seems reasonable to postulate that if *impurity* scattering of the s-d type is an important process, then so also are *phonon-induced* s-d processes, in which case the $n(E_F)$ of Eq. (2) may again be regarded as the total $(s+d)$ state density. Some standard texts (e.g., Refs. 26–28) show that at "high temperatures",[29] $1/\Lambda_i \propto T/\Theta_D^2$. Thus, at some constant high temperature,

$$\rho_i \propto n(E_F)/n\Theta_D^2\ . \tag{3}$$

According to the Hall-effect studies of Hake *et al.*,[2] the electron density n in β-Ti-Mo is independent of solute concentration. We need, therefore, only concern ourselves with the variations of $n(E_F)$ and Θ_D with composition. From low-temperature specific-heat and magnetic susceptibility measurements[22] performed on a Ti-Mo (0–100-at.%) series, a set of values of $n(E_F)$ and Θ_D has been obtained for alloys possessing the "as-quenched" structures described in Fig. 1(c). In addition, with the aid of some extrapolation procedures, we

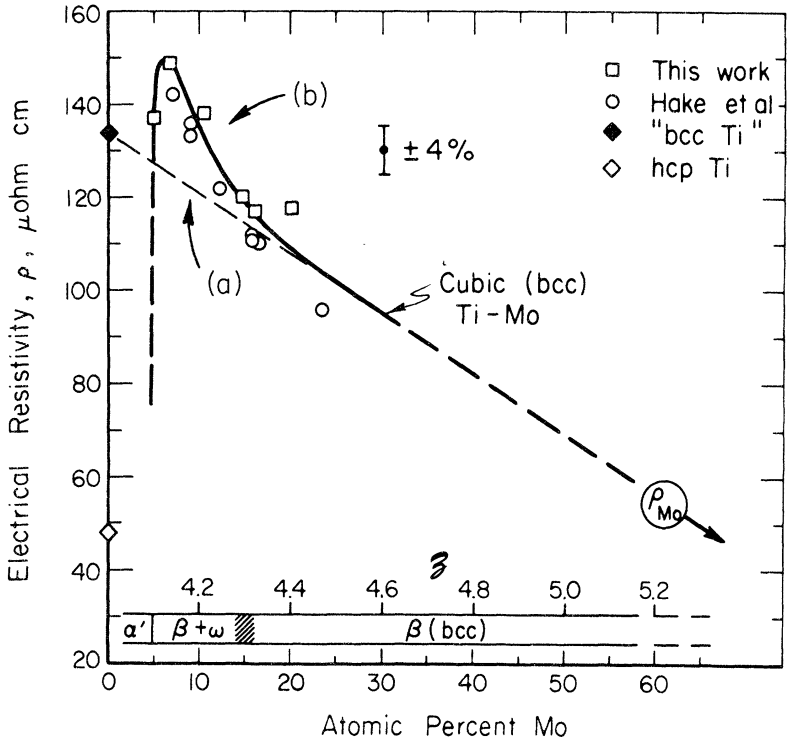

FIG. 4. Resistivity composition dependence in Ti-Mo, indicating the two different classes of evidence produced by earlier workers in support of the existence of a negative $d\rho/dc$ in β-Ti-Mo. (a) A line, connecting the literature-estimated ρ_i(300 K) for pure β-Ti with ρ_i(300 K) for pure Mo, passes near some data points corresponding to ρ_i(β-Ti-Mo, 300 K), and has a negative slope. (b) The focusing of attention onto ρ-c in a suitably limited concentration range suggests the existence of a negative $d\rho/dc$.

have derived $n(E_F)$ and Θ_D values for single-phase β-Ti-Mo (5–15 at.%), assuming it to exist at ordinary temperatures unperturbed by the presence of ω phase. These data are listed in Table II. On the preliminary assumption that $\rho = \rho_i + \rho_s$, the resistivities of β-phase and ($\beta + \omega$)-Ti-Mo alloys are calculated using the proportionalities (1) and (3).

2. *Preliminary Calculation Based Primarily on an Estimated Room-Temperature Resistivity for β-Ti*

As indicated in Sec. III A the results of previously reported experiments[5,19] have suggested that the ideal resistivity at 300 K of the cubic allotrope of pure Ti, if it existed at room temperature, would be about 134 $\mu\Omega$cm. Indeed such a high resistivity for β-Ti, as well as for virtual β-Ti-Mo alloys, would be consistent with the relatively low Debye temperatures estimated for these materials (Table II). In this preliminary resistivity calculation we formed equalities from (1) and (3) by setting ρ_i(β-Ti, 300 K) = 134 $\mu\Omega$cm, and by using the measured value ρ(TM-20, 300 K) = 118 $\mu\Omega$cm. The components ρ_s and ρ_i were then calculated for all the alloys. For TM-20, in particular, we found ρ_i = 41 $\mu\Omega$cm, from which it follows that ρ_s = 77 $\mu\Omega$cm. Calculated values of ρ_s and ρ for the alloy series (0–70 at.%) are shown in Fig. 5.

In that figure the relatively small Θ_D values

TABLE II. Values of $n(E_F)$ and Θ_D for bcc Ti-Mo alloys, derived from magnetic susceptibility and calorimetric experiments, either directly (D), or by extrapolation (X). The derivation of these quantities has been discussed in a separate paper by the present authors (Ref. 22). The microstructures of the alloys in columns D are successively β (pure Mo to TM-20) and $\beta + \omega$ (TM-15 to TM-5); while for columns X (TM-15 to TM-5), the structure is designated "virtual bcc," a terminology which we have used to indicate instability of the single-phase bcc lattice at ordinary temperatures.

Alloy	Density of states $n(E_F)$ (eV atom)$^{-1}$ D	X	Debye temp. Θ_D (K) D	X
Pure Mo	0.35_6	···	470[a]	···
TM-70	0.49_0	···	410	···
TM-40	0.97	···	365	···
TM-25	1.07	···	320	···
TM-20	1.08	···	305	···
TM-15	1.10	1.13	295	281
TM-10	1.06	1.22	320	243
TM-8½	0.97	1.25	320	232
TM-7	0.89	1.30	350	220
TM-5	0.75	1.35	380	207
β-Ti	···	1.50	···	200[b]

[a]After F. J. Morin and J. P. Maita, Phys. Rev. 129, 1115 (1963).

[b]We regard β-Ti as "absolutely unstable" at ordinary temperatures.

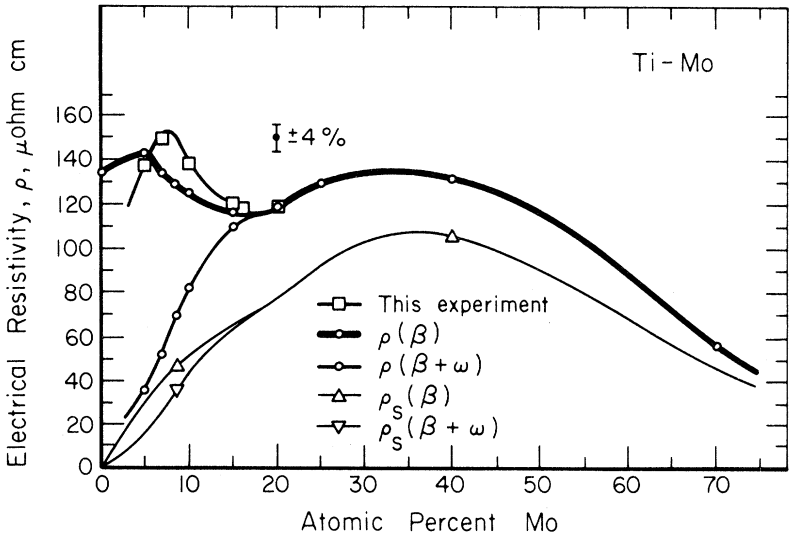

FIG. 5. Calculated resistivities $\rho(=\rho_i+\rho_s)$ and ρ_s, where $\rho_i \propto n(E_F)/\Theta_D^2$ and $\rho_s \propto n(E_F)c(100-c)$; using as "boundary conditions" $\rho_i(\beta$ Ti, 300 K) = 134 $\mu\Omega$ cm and ρ(TM-20, 300 K) = 118 $\mu\Omega$ cm. A maximum, approximating that observed experimentally, is fortuitously reproduced by the calculated $\rho(\beta)$ curve.

which Table II assigns to "virtual" β-Ti-Mo have resulted in enhanced values of ρ_i, and hence total resistivity ρ, throughout the concentration range 0–15 at.% Mo. In fact, if a possible ± 4% experimental scatter is taken into account, there is reasonably good agreement between the experimental data and the calculated $\rho(\beta)$ curve. However, although it is certainly appropriate to assign low Θ_D values to low-concentration virtual β-Ti-Mo alloys, a procedure which leads to enhanced ideal resistivities for such alloys, the above analysis is not a valid interpretation of the *observed* resistivity anomaly for the following reasons: (a) The analysis leads to $\rho_i/\rho_s = 41/77$ for TM-20 at 300 K, whereas experimentally (cf. Table I) we found ρ_i/ρ_s (300 K) $=\frac{8}{110}$. (b) The

TABLE III. Estimated total resistivities ρ and resistivity components ρ_i and ρ_s for β-phase and $(\beta+\omega)$-phase Ti-Mo alloys, computed from empirical values of $n(E_F)$ and Θ_D.

Alloy	Analyzed composition (at.% Mo)[a]	Density of states for single spin direction $n(E_F)$ (eV atom)$^{-1}$		Debye temp. Θ_D (K)		Ideal resistivity $\rho_i \propto n(E_F)/\Theta_D^2$ set at 8 μΩ cm for TM-20 (300 K)		Solute scattering resistivity $\rho_s \propto n(E_F)c(100-c)$ set at 110 μΩ cm for TM-20		Total resistivity at 300 K $\rho=\rho_i+\rho_s$ (μΩ cm)	
		β[b]	$\beta+\omega$	β	$\beta+\omega$	β	$\beta+\omega$	β	$\beta+\omega$	β	$\beta+\omega$
β-Ti	0	1.50	···	200	···	25.8	···	0	0	25.8	···
TM-5	5.16	1.35	0.75	207	380	21.7	3.6	43.1	23.9	64.8	27.5
TM-7	6.96	1.30	0.89	220	350	18.5	5.0	54.9	37.6	73.4	42.6
TM-8½	8.86	1.25	0.97	232	320	16.0	6.5	65.8	51.1	81.8	57.6
TM-10	10.30	1.22	1.06	243	320	14.2	7.1	73.5	63.8	87.7	71.0
TM-15	14.92	1.13	1.10	281	295	9.9	8.7	93.5	91.0	103.4	99.7
TM-20[c]	19.38	1.08	···	305	···	8.0	···	110.0	···	118.0	···
TM-25	25.36	1.07	···	320	···	7.2	···	132.0	···	139.2	···
TM-40	39.81	0.97	···	365	···	5.0	···	151.5	···	156.5	···
TM-70	71.02	0.49_0	···	410	···	2.0	···	65.7	···	67.8	···
Pure Mo	100	0.35_6	···	470[d]	···	1.1	···	0	···	1.1	···

[a]Compositions of specific-heat ingots which yielded the $n(E_F)$ and Θ_D data.

[b]Only the quenched alloys TM-(20–100) are stable bcc at room temperature. We refer to bcc TM (5–15) as "virtual bcc" and β-Ti as "absolutely unstable."

[c]Calculated resistivities fitted to values of ρ_i and ρ_s for TM-20.

[d]After F. J. Morin and J. P. Maita, Phys. Rev. 129, 1115 (1963).

microstructures of the alloys which exhibit the anomaly are two-phase $\beta+\omega$ rather than single-phase β.

3. *Final Resistivity Calculation Based on the Measured ρ and $d\rho/dT$ for TM-20*

In this analysis we convert (1) and (3) into equalities with constants derived using the results of the resistivity experiments on the single-phase bcc as-quenched alloy TM-20, for which $\rho_i(300\ \mathrm{K}) = 8\ \mu\Omega\,\mathrm{cm}$, and $\rho_s = 110\ \mu\Omega\,\mathrm{cm}$ (Table I). The resistivity components for the alloy series, calculated using (1) and (3) and the above boundary values, are listed in Table III. They are also

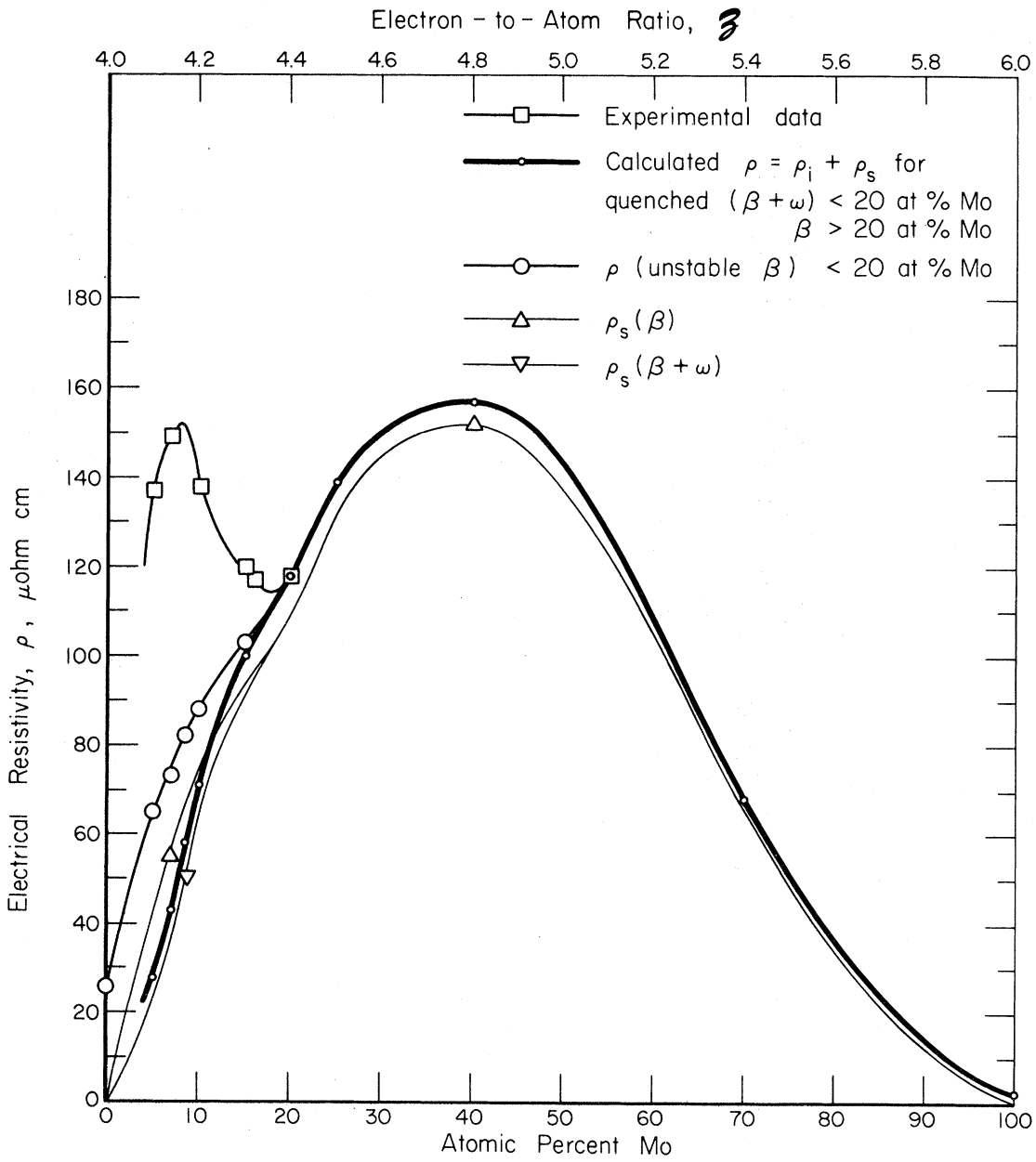

FIG. 6. Calculated resistivity composition dependence in Ti-Mo from the data of Table III. The principal calculated curve (heavy line), which has the usual distorted parabolic shape, represents $\rho=\rho_i+\rho_s$ for as-quenched $(\beta+\omega)$-phase and β-phase Ti-Mo in the appropriate concentration ranges. A curve representative of ρ (unstable β) for <20 at.% Mo is included for comparison. The figure shows that the measured resistivities of alloys in the compositional range 5–15 at.% Mo are anomalously high by comparison with the calculated $\rho(\beta+\omega)$ [which actually lies *below* that of the calculated $\rho(\beta)$], and cannot, therefore, be described in terms of the usual two-component $(\rho=\rho_i+\rho_s)$ model.

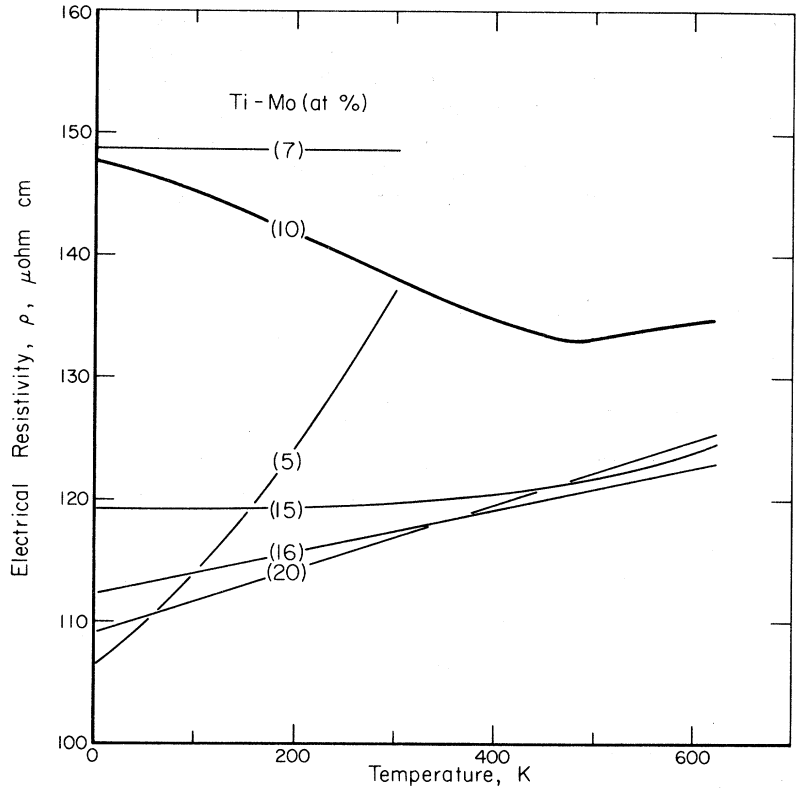

FIG. 7. Temperature dependences of resistivity for six Ti-Mo alloys. TM-10 shows a negative $d\rho/dT$ in the range 4–480 K, while the alloys on either side of it in composition have resistivities practically independent of temperature in the 4–300-K range. TM-10 exhibits normal $d\rho/dT$ behavior above 480 K.

displayed in Fig. 6, where it can be seen that the composition dependence possesses the frequently encountered distorted parabolic shape. The figure also shows that the *measured* resistivities (0–15 at.% Mo) are greatly in excess of the calculated quantities, the experimental curve peaking at a resistivity value some 70–80 $\mu\Omega$cm higher than that derived using the two-component ($\rho = \rho_i + \rho_s$) model. It is important to note that, as in the previous calculation, $\rho(\beta+\omega)$ is *less* than $\rho(\beta)$, since one of the effects of ω-phase precipitation is to lower the average $n(E_F)$.[14,22] Thus, although we suspect that the presence of ω phase is the source of the anomalous resistivity, its introduction, within the framework of a two-component $\rho_i + \rho_s$ model, is completely incapable of leading to the measured resistivity values. Clearly, an additional resistivity component is required to explain the observed effect. Since the anomaly occurs within the $\beta+\omega$ field, and the microscopic results of the presence of ω phase have already been taken into consideration [through $n(E_F)$ and Θ_D], we suggest that the excess resistivity is due to a kind of defect scattering ρ_{def} occurring at the interfaces between the matrix and the partially coherent ω-phase precipitates. As will be discussed in Sec. III C, a model based on interfacial scattering also leads to an explanation of the observed negative $d\rho/dT$.

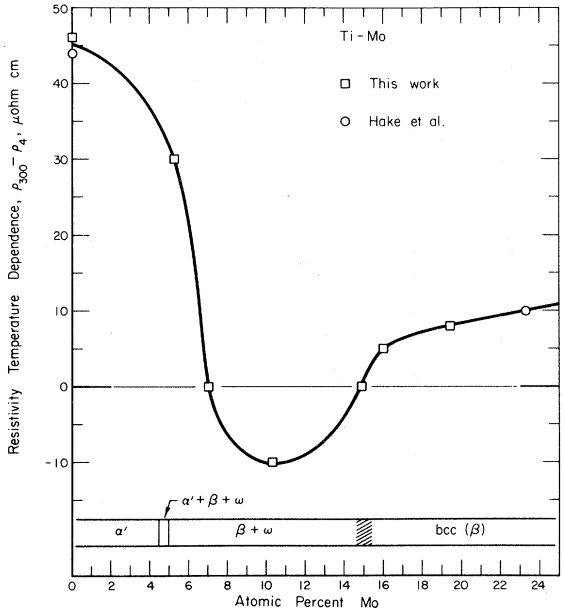

FIG. 8. Relative resistivity temperature dependences ($\rho_{300K} - \rho_{4K}$) of Ti-Mo alloys. The figure shows clearly that negative $d\rho/dT$ is confined to those alloys whose quenched microstructures are $\beta+\omega$. Open circles represent the work of Hake *et al.* (Ref. 2); with regard to which we note that, although the absolute resistivity of their Ti-Mo (23-at.%) sample seemed out of line compared to our results (Fig. 2), the temperature dependence is in excellent accord.

C. Temperature Dependences of Resistivity of the Ti-Mo Alloys

The resistivity temperature dependences of the five alloys are shown in Fig. 7. Of particular interest are the negative $d\rho/dT$ for TM-10, and the zero $d\rho/dT$'s (0–300 K) for the pair of alloys bracketing it in composition. The composition dependence of $d\rho/dT$ is shown explicitly in Fig. 8. There we see that negative $d\rho/dT$ is confined to the $\beta+\omega$ regime, the largest negative value occurring at 10 at.% Mo. For compositions near that value the ω-phase precipitation present in the as-quenched ingots, although dense, has not proceeded to completion.

Figure 8 emphasizes the existence of a close connection between the occurrence of negative $d\rho/dT$ and ω-phase precipitation. Even so, a static assembly of macroscopic precipitates[30] is unable to yield a negative-temperature-dependence mechanism. At this point it is instructive to notice that in TM-10 the ρ_{def} resistivity component is 67 $\mu\Omega$cm, compared to which the increase in resistivity between 300 and 4 K (viz., 10 $\mu\Omega$cm) is relatively small. If, therefore, we ascribe the room-temperature excess resistivity to interfacial scattering between matrix and precipitate, only a slight increase in precipitate abundance with decreasing temperature would satisfy the observed $d\rho/dT$. Since the resistivity temperature dependence was apparently insensitive to thermal cycling between 4 and 300 K, any additional precipitation of this kind would need to be reversible. However, it would be difficult to postulate such a requirement in the absence of some other experimental evidence in support of the occurrence of reversible ω-phase precipitation in Ti-Mo.

1. Reversible ω-Phase Precipitation in Ti-Mo

In a recent discussion of ω-phase transformations in Ti alloys, de Fontaine, Paton, and Williams[31] have demonstrated that in a very rapidly quenched Ti-Mo (8-at.%) alloy ω phase will precipitate diffusionlessly as the cooling is continued into the liquid-nitrogen temperature range, and that the process is completely reversible under

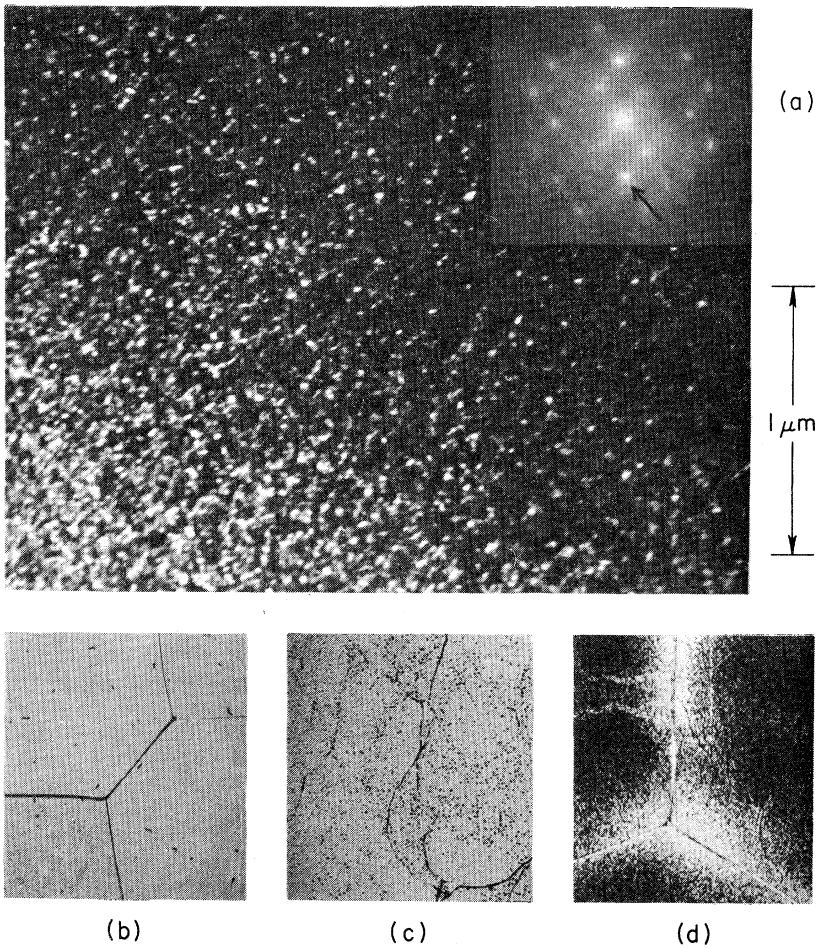

FIG. 9. (a) Dark-field electron micrograph of a specimen taken from an ice-brine-quenched 30-g ingot of TM-10. The arrow in the inset points to the corresponding electron-diffraction spot originating from the ω phase. This initial ω phase, which appears during the relatively slow ice-brine quenching of a massive ingot, is chiefly of the "isothermal" type. (b)–(d) are optical photomicrographs (originally × 300) showing the development of ω-phase precipitation after successive agings of 1 h at 300 °C, 8 h at 350 °C, and 150 h at 350 °C. Experiments described in the literature (Refs. 7, 10, 35) and others performed in this laboratory (Ref. 34) prove conclusively that we are seeing a development of ω phase precipitation, rather than a decomposition into the equilibrium $(\alpha+\beta)$.

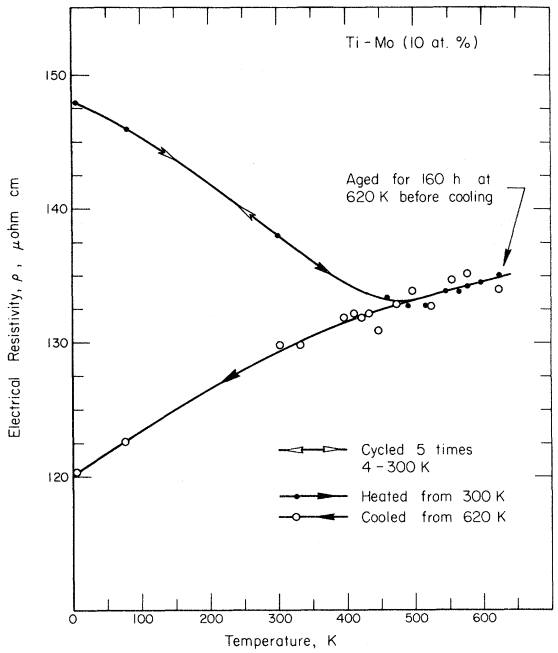

FIG. 10. Resistivity temperature dependence in TM-10 before and after aging. The negative $d\rho/dT$ is ascribed to the dissolution of reversible (athermal) ω phase with increasing temperature. The aging heat treatment, accompanied by a development of irreversible (isothermal) ω, removes the possibility of reprecipitation of athermal ω during a return to low temperatures. As a consequence, the aged alloy possesses a normal resistivity temperature dependence. The constancy of ρ(TM-10) during aging at 620 K is discussed in the text.

thermal cycling. A small hysteresis in precipitate abundance versus temperature (corresponding to 10–15 °C) which they observed should be detectable resistometrically if readings are taken at sufficiently close temperature intervals. In our TM-10 alloy, ω phase was already present after the relatively slow quench into iced brine [Fig. 9(a)]. However, we suggest (a) that although this consisted chiefly of an irreversible ("isothermal") precipitate, a small fraction of the as-quenched ω phase was in fact of the reversible ("athermal") kind referred to above, and as such was able to dissolve during the heating to 480 K (Fig. 7); (b) furthermore, that the cooling below room temperature resulted in the precipitation of additional athermal ω phase, within the previously untransformed β matrix.[32]

2. *Influence of Aging on the ω-Phase Precipitate and Resistivity Temperature Dependence in TM-10*

Figure 9 shows what appears to be the development[33] of the ω-phase precipitate in TM-10 during aging at 620 K. Experiments to be reported elsewhere[34] have proved beyond doubt that the microstructural change seen represents ω-phase development, rather than α-phase precipitation. In order to induce the reaction $\beta+\omega \rightarrow \alpha+\beta$ within a reasonable time scale it is necessary to anneal at somewhat higher temperatures (e.g., 820 K).[7,10,34,35]

After the aging at 620 K the alloy assumed a normal resistivity temperature dependence (Fig. 10). This result, taken with the observations of Williams *et al.*,[31] who reported that the heating of Ti-Mo (8 at.%) to 570 K resulted in the transformation of athermal to isothermal ω phase (a process which they suggested was brought about by a diffusion-controlled composition change of the kind discussed by Hickman[8]), lends strength to the argument that the negative $d\rho/dT$ observed in the as-quenched alloys was due to the presence of a small fraction of athermal ω.

Finally, it is interesting to speculate upon the reason for the negligible change of resistivity during heat treatment at 620 K. This null effect results from the operation of a pair of compensatory mechanisms. On the one hand, precipitate development is accompanied by an *increase* in interfacial area and consequently ρ_{def}. On the other, it is responsible for a *reduction* in $\langle n(E_F)\rangle_{av}$[14,34] to which the other resistivity components ρ_i and ρ_s are both proportional.

IV. SUMMARY

The *concentration dependence* of resistivity of a series of Ti-rich Ti-Mo alloys was found to possess a pronounced local maximum near 8 at.% Mo, i.e., well within the $\beta+\omega$ regime for quenched 30-g ingots. Comparison with theory showed that this excess resistivity could not be accounted for in terms of normal solute or thermal scattering in the $(\beta+\omega)$-phase and β-phase material, but that an additional term ρ_{def} due to matrix-precipitate interfacial scattering was required to satisfy the observations. The *negative temperature dependence* of resistivity exhibited by one of the alloys (TM-10) within the $\beta+\omega$ region could be accounted for in terms of a negative $d\rho_{def}/dT$ due to the reversible precipitation of a small volume fraction of athermal ω phase, the possibility of the existence of which has been substantiated by direct microstructural studies carried out elsewhere.[31] Finally, the saturation of ω-phase precipitation in TM-10 by aging at 620 K prevented the subsequent formation of athermal ω phase during cooling to room temperature and below, thus conferring on that alloy a normal positive resistivity temperature dependence.

ACKNOWLEDGMENTS

We thank Dr. D. de Fontaine, Dr. N. E. Paton, and Dr. J. C. Williams for discussing their work

with us and Dr. Paton for a helpful suggestion with regard to the possible role of athermal ω phase in resistivity temperature dependence; also Dr. J. D. Boyd and C. J. Martin, who helped with the electron microscopy of several of the Ti-Mo specimens, and R. D. Smith for technical assistance (magnetic susceptibility and optical metallography).

---

*Work supported by Battelle, Columbus Laboratories and the Air Force Materials Laboratory, Wright-Patterson Air Force Base, Ohio, for financial support.

†Present address: Physics Department, Wichita State University, Wichita, Kans. 67208.

[1]S. Yoshida and Y. Tsuya, J. Phys. Soc. Japan 11, 1206 (1956).

[2]R. R. Hake, D. H. Leslie, and T. G. Berlincourt, J. Phys. Chem. Solids 20, 177 (1961).

[3]F. R. Brotzen, E. L. Harmon, and A. R. Troiano, Trans. AIME 203, 413 (1955).

[4]T. S. Luhman, R. Taggart, and D. H. Polonis, Scripta Met. 2, 169 (1968).

[5]S. L. Ames and A. D. McQuillan, Acta Met. 2, 831 (1954).

[6]D. J. Cometto, G. L. Houze, and R. F. Hehemann, Trans. Met. Soc. AIME 233, 30 (1965).

[7]M. J. Blackburn and J. C. Williams, Trans. Met. Soc. AIME 242, 2461 (1968).

[8]B. S. Hickman, J. Inst. Metals 96, 330 (1968).

[9]B. S. Hickman, J. Mater. Sci. 4, 554 (1969).

[10]B. S. Hickman, Trans. Met. Soc. AIME 245, 1329 (1969).

[11]The electrorefined Ti sponge, grade ELXX from the Titanium Metals Corporation, contained as principal impurities in weight percent O_2, 0.037; N_2, 0.004; Cl_2, 0.073; and Fe, 0.009. The Mo, from Climax Molybdenum Co., contained as principal impurities in weight percent C, 0.014; O_2, <0.0004; H_2, <0.0001; N_2, <0.0001; Fe, <0.006; Ni, <0.001; Si, <0.002.

[12]E. W. Collings and J. C. Ho, in *The Science, Technology, and Application of Titanium*, edited by R. I. Jaffee and N. E. Promisel (Pergamon, New York, 1970), p. 331.

[13]J. C. Ho and E. W. Collings, Phys. Letters 29A, 206 (1969).

[14]E. W. Collings and J. C. Ho, in *Proceedings of the Third Materials Research Symposium*, 1969, Natl. Bur. Std. (U.S.) Spec. Publ. 323 (U. S. GPO, Washington, D.C., 1971), p. 587.

[15]E. W. Collings and J. C. Ho, Phys. Letters 29A, 306 (1969).

[16]E. W. Collings and J. C. Ho, Phys. Rev. B 1, 4289 (1970).

[17]J. C. Ho and E. W. Collings, J. Appl. Phys. 42, 5144 (1971).

[18]Value derived graphically from a photographic enlargement of Fig. 1 of Ref. 5.

[19]R. J. Wasilewski, Trans. Met. Soc. AIME 224, 5 (1962).

[20]Obtained by combining the 41 $\mu\Omega$ cm at 273 K of Ref. 2 with a temperature dependence at 300 K of 0.22 $\mu\Omega$ cm/deg from Ref. 19.

[21]The present specimens were annealed in the bcc field and ice-brine quenched, while those of Ref. 2 had been measured in the "as-cast" condition.

[22]E. W. Collings, J. C. Ho, and R. I. Jaffee, Phys. Rev. B 5, 4435 (1972).

[23]N. F. Mott and H. Jones, *The Theory of Properties of Metals and Alloys* (Dover, New York, 1958), p. 300.

[24]B. S. Chandrasekhar and J. K. Hulm, J. Phys. Chem. Solids 7, 259 (1958).

[25]R. R. Hake, Phys. Rev. 123, 1986 (1961).

[26]G. K. White, *Experimental Techniques in Low-Temperature Physics* (Oxford U.P., Oxford, England, 1959), Chap. XI.

[27]J. M. Ziman, *Principles in the Theory of Solids* (Cambridge U.P., Cambridge, England, 1965), pp. 188–192.

[28]G. T. Meaden, *Electrical Resistance of Metals* (Pergamon, New York, 1965), p. 98.

[29]The high-temperature regime is certainly that for which T/Θ_D is large (Ref. 26); however, the T/Θ_D^2 relationship seems to be valid in the intermediate temperature range down to $T/\Theta_D \sim 0.5$ (Ref. 26).

[30]With a mean free path of about 5 Å, the conduction electrons see a macroscopic two-phase mixture.

[31]D. de Fontaine, N. E. Paton, and J. C. Williams, Acta Met. 19, 1153 (1971).

[32]We are grateful to Dr. N. E. Paton for this suggestion.

[33]By "development" we imply some precipitation growth, of unspecified extent, together with some diffusion-induced compositional changes. For details on the influence of aging an ω-phase precipitate development, see, for example, Refs. 8–10.

[34]E. W. Collings and J. C. Ho (unpublished).

[35]J. C. Williams, B. S. Hickman, and H. L. Marcus, Met. Trans. 2, 1913 (1971).

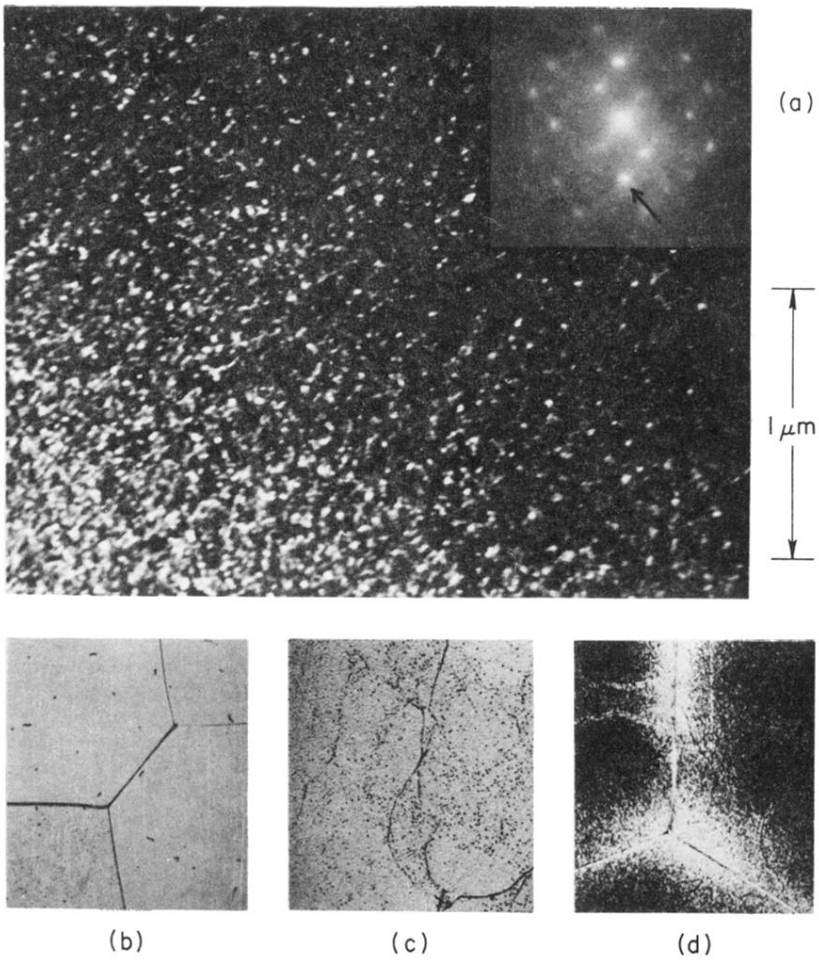

FIG. 9. (a) Dark-field electron micrograph of a specimen taken from an ice-brine-quenched 30-g ingot of TM-10. The arrow in the inset points to the corresponding electron-diffraction spot originating from the ω phase. This initial ω phase, which appears during the relatively slow ice-brine quenching of a massive ingot, is chiefly of the "isothermal" type. (b)–(d) are optical photomicrographs (originally $\times$ 300) showing the development of ω-phase precipitation after successive agings of 1 h at 300 °C, 8 h at 350 °C, and 150 h at 350 °C. Experiments described in the literature (Refs. 7, 10, 35) and others performed in this laboratory (Ref. 34) prove conclusively that we are seeing a development of ω phase precipitation, rather than a decomposition into the equilibrium $(\alpha + \beta)$.